Hidden variety of biotin–streptavidin/avidin local interactions revealed by site-selective dynamic force spectroscopy

Atsushi Taninaka, Osamu Takeuchi and Hidemi Shigekawa*

By site-selective dynamic force spectroscopy realized with the combination of cross-linkers and anatomic force microscope with a force feedback system, we have revealed, for the first time, that the slight difference between the local structures of amino acid residues at the middle sites, SER45 and THR35 for streptavidin and avidin, respectively, strongly affects the microscopic reaction processes, *i.e.*, the variation governs the type of bond as well as the fine structure of the potential landscape. For streptavidin, a bridged or direct hydrogen bond is induced depending on the molecular structure in the buffer solution. For avidin, in contrast, only a direct hydrogen bond is observed for all the buffer solutions used in the experiment. Since final functions in a system are realized through the assembly of local effects, the obtained results indicate the importance of analyzing the reaction processes with respect to the local structures of molecules, for further development of nanoscale functional devices.
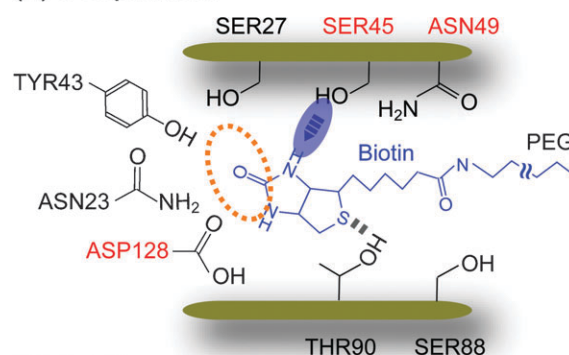
1. Introduction

The specific natures of functional molecules are governed by the characteristics of their local structures and properties in many cases.[1–4] In fact, even in the reaction dynamics of complex materials such as proteins, a variety of local structures, for example, affect the steric hindrance of enzyme reactions;[1–3] thereby, they play an important role in governing total reaction processes. Therefore, for further understanding of molecular recognition properties and their application to the development of functional devices, it is of great importance to analyze the reaction processes of molecules with respect to a variety of local structures and their properties. However, such an analysis has not been successfully carried out because of the difficulty in discriminating the characteristics of the selected site from complex interactions.

To investigate the microscopic processes, we performed site-selective dynamic force spectroscopy (DFS)[5–28] on typical ligand and receptor, namely, streptavidin/avidin–biotin systems. Site-selective DFS is the method which enables us to investigate the site-dependent stochastic process of a chemical reaction of molecules at the single-molecule level.[23,24]

Fig. 1 shows schematics of the bonding structures of streptavidin/avidin–biotin systems.[1–3] As is shown in Fig. 1(a), the binding pocket of streptavidin has several reaction sites with a hydrogen-bonding network, which are classified into the following three groups depending on the distance from the bottom of the binding pocket: (1) inner binding sites of amino acid residues SER27, ASN23, TYR43 and ASP128, (2) middle binding sites SER45 and THR90, and (3) outer sites ASN49 and SER88.[1,2] On the other hand, as shown by the schematic structure of the avidin molecule in Fig. 1(b), avidin has three amino acid residues that are different from those in streptavidin.[3]

*Institute of Applied Physics, CREST-JST, University of Tsukuba, 1-1-1 Tennodai, Tsukuba, Ibaraki, Japan.
E-mail: hidemi@ims.tsukuba.ac.jp; Web: http://dora.ims.tsukuba.ac. jp/; Fax: +81-29-853-5276; Tel: +81-29-853-5276*
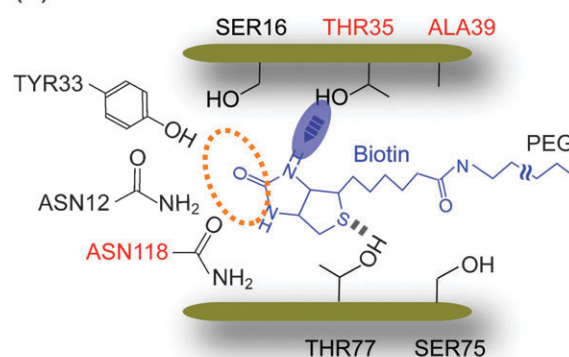

Fig. 1 Schematics of the bonding structures of (a) streptavidin–biotin and (b) avidin–biotin complexes. Three different sites are indicated by red letters. Orange dotted and blue circles indicate the inner and middle binding sites discussed in text.

Although notable difference in the characteristics of two molecules for chemical reactions cannot be probed by thermodynamic method, the local variations between streptavidin and avidin may provide a difference hidden behind the averaged function when microscopic potential landscapes are directly

probed. In fact, in the pioneering work[7,8] by DFS on these materials, although details could not be clarified in an ordinary way, a slight difference in the value of potential positions was observed between biotin/streptavidin (0.5 nm) and biotin/avidin structures (0.3 nm). Furthermore, in a previous paper, it was reported that reaction sites of streptavidin and biotin form a bridged bond in 0.01 M phosphate (pH 7.4), while they form a direct hydrogen bond in 0.05 M sodium nitrate (pH 7),[23–25] suggesting a significant effect of ion species in buffer solutions on the bond formation, which may also result in a different bond formation for avidin. Therefore, probing to obtain a deeper understanding of these typical ligand–receptor systems is of great importance for providing a general basis for designing and controlling the mechanism of chemical reactions between two more complicated functional molecules.

Using site-selective DFS, effects of the local variation in the type of amino acid residues in streptavidin and avidin molecules on their reaction dynamics with a biotin molecule were studied in detail at the single molecular level, and critical effects, which had been hidden behind the averaged function, were revealed, for the first time.

2. Experimental

2.1 Sample preparation and buffer solutions

Fig. 2(a) shows a schematic illustration of a sample preparation. A gold-coated cantilever (Bio-Lever, Olympus, 6 pN nm^{-1}
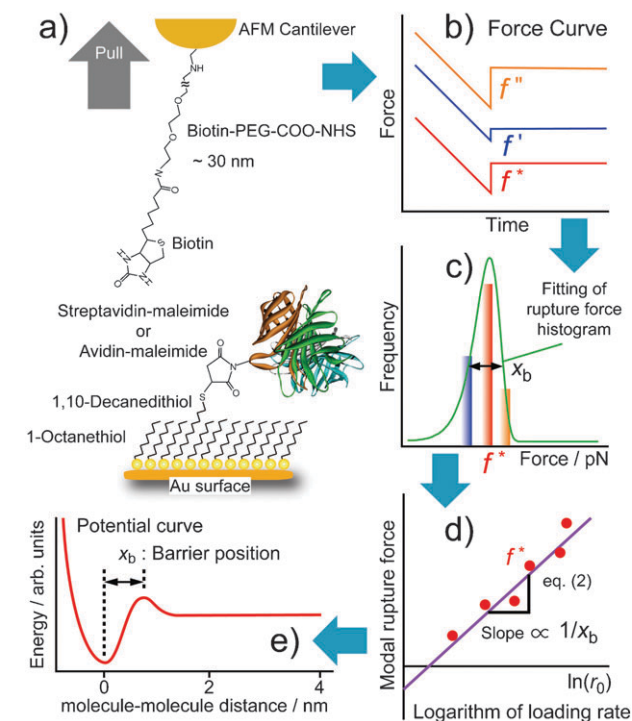

Fig. 2 (a) Schematic illustrations of the apex of a modified cantilever. Streptavidin or avidin is fixed to a SAM of 1,10-decanedithiol/1-octanethiol (1/100 ratio) mixed solution on a Au-coated substrate *via* a streptavidin–maleimide or avidin–maleimide structure. (b)–(d) Procedures of obtaining potential barrier position shown in (e).

and 30 pN nm^{-1}, rectangular shape) was immersed into a solution of 8-amino, 1-octanethiol hydrochloride molecules (1 mM in ethanol) for 48 h to form a closely packed self-assembled monolayer (SAM) with amino groups on the surface. After rinsing with ethanol, the cantilever was immersed into a solution of biotin-PEG3400-COO-NHS molecules (Shearwater Polymers, 0.1 mM in ethanol) for 20 h to fix a biotin (biotin-PEG) molecule onto the probe apex. Finally, the cantilever was rinsed with ethanol.

For probing middle sites selectively, streptavidin/avidin molecules were fixed *via* a streptavidin–maleimide or an avidin–maleimide structure on the substrate.[23,24] First, as a substrate, a thin gold film (100 nm) was evaporated onto a freshly cleaved mica surface in a high vacuum at 400 °C and flame-annealed using a hydrogen gas burner for 30 s. Then, the substrate was immersed into a solution of 1,10-decanedithiol/1-octanethiol (1/100 ratio) (1 mM in ethanol) for 48 h to form a closely packed SAM with thiol groups on the surface. The substrate was immersed into a solution of streptavidin–maleimide (10 mg l^{-1} in phosphate-buffered saline (PBS) (pH 7.4) : N,N-dimethylformamide = 99 : 1) for 5 h to fix streptavidin molecules to the substrate. The avidin–maleimide was synthesized using avidin molecules (1 mg ml^{-1} in phosphate-buffered saline (PBS)) and a sulfo-SMCC of 0.1 mg, and the activated avidin was purified by desalting on a column and an HPLC (High performance liquid chromatography). The formation of closely packed SAMs on the probe apex and substrate was necessary to decrease the strong interaction between the gold layers on both surfaces.

To avoid multiple-bonding events, as mentioned above, the density of the target molecules in the SAM was reduced so that the probability of bonding became 5–10% for each tip–sample approach. Furthermore, only single ruptures were counted to remove the errors caused by the effect of multiple-rupture events on the analysis.

For buffer solutions, in addition to 0.01 M phosphate (pH 7.4) and 0.05 M sodium nitrate (pH 7), which were used in previous studies of streptavidin,[23–25] we prepared 0.05 M carbonate (pH 10) that has a structure similar to that of sodium nitrate but has a different pH.

2.2 Measurement procedures

In DFS, the unbinding force applied to a molecular pair is increased at a constant rate, and the force required to rupture the bond is measured. Through the analysis of the relationship between the modal rupture force and the logarithm of the loading rate, microscopic potential barrier landscapes (distance from the potential minimum) and the lifetimes of bonds can be obtained.[5–28] The lifetime of a molecular bond is dependent on potential barrier height. When a tensile force is applied to a bond, the potential landscape is deformed; thus, barrier height decreases. For a constant loading rate of the tensile force, the probability distribution of the rupture force can be expressed as

$$P_{(f)} = C \exp\left\{\frac{(f - f^*)x_b}{k_B T}\right\} \exp\left[1 - \exp\left\{\frac{(f - f^*)x_b}{k_B T}\right\}\right] \quad (1)$$

where $P_{(f)}, f, f^*, x_b, k_B, T$, and C are the probability distribution of the rupture force, the rupture force, the modal rupture force, the potential barrier position, the Boltzmann constant, the temperature and a constant, respectively.[7,8,23–25] According to eqn (1), f^* linearly depends on the logarithm of the loading rate $r_0((= df/dt))$ as shown by

$$f^* = \frac{k_B T}{x_b}\left\{\ln r_0 + \ln\left(\frac{t_{\text{off}(0)}x_b}{k_B T}\right)\right\} \quad (2)$$

where $t_{\text{off}(0)}$ is the lifetime of a molecular bond. Eqn (2) indicates that the potential barrier position can be obtained from the slope of the linear relationship.[5–28]

When using eqn (1) or (2), it is essential to maintain a constant loading rate.[13,14,23–27] When the DFS measurement is carried out by an atomic force microscope (AFM) with a cross-linker molecule, however, a constant retraction velocity does not result in a constant loading rate because of the stretching of the cross-linker molecule. Namely, controlling of the applied force to maintain a constant loading rate is of great importance. An AFM system with a feedback loop was used to satisfy this requirement,[23–27] which enables the fine control of low loading rates to reduce the effect of the soft cross-linker that connects a sample molecule to the tip.[23–27] The AFM system also enables us to realize a high sampling rate (100 kHz) to obtain a sufficient amount of data at a high loading rate.[23–25] Furthermore, since AFM measurement is stable under various buffer solutions, different buffer solutions with different pH values can be used.

For a selected loading rate, many rupture forces are measured from force curves (Fig. 2(b)). The measured rupture forces are shown in a histogram, from which the modal rupture force is obtained for each loading rate measurement by theoretical fitting (Fig. 2(c)). Then, the modal rupture force is plotted as a function of the logarithm of the loading rate (Fig. 2(d)): therefore, information concerning the energy landscape of the interaction is derived from the relationship between the modal rupture force obtained from the histogram and the loading rate of the unbinding force. In addition, the width of the histogram also provides the potential barrier position by analysis using eqn (1), which can be used to examine the validity of the results obtained from the slope shown in Fig. 2(d).

For our experiment, the loading rate was controlled between 10 and 10^5 pN s^{-1}, and 5000–10 000 approach and retract cycles were carried out to form a histogram for each loading rate measurement.

3. Result and discussion

Fig. 3(a) and (b) show two different forms of a typical force curve obtained using the system that we developed[23–25] as functions of (a) distance and (b) time. The distance represents the length of the cantilever retraction after zero force was measured. Since the cantilever was moved in until the force reached 50 pN for setup, there exists a negative region for the distance. Although the force does not show a linear change in (a) owing to the existence of a PEG molecule, a linear change is shown in (b). This result also indicates that a constant
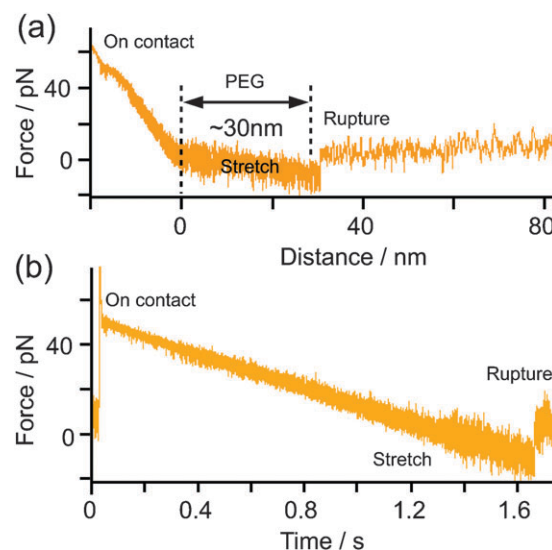

Fig. 3 Two different forms of a typical force curve obtained using the system that we developed[23–25] as functions of (a) distance and (b) time.

loading rate is achieved using the AFM system that we developed.

When a molecular cross-linker is used to fix a sample to a tip, the condition of a constant loading rate cannot be satisfied. By considering the effect, several models have been proposed.[13–22] However, since the AFM system with a feedback loop that we used satisfies the condition of a constant loading rate, the effect of the soft cross-linker that connects a sample molecule to the tip can be satisfactorily minimized. Therefore, eqn (1) and (2) of the Bell–Evans model can be used without any modifications for the analysis of the obtained results.[21–25]

As described in the Experimental section, for a selected loading rate, many rupture forces were measured from force curves. The rupture forces were summarized in a histogram, from which the modal rupture force was obtained for each loading rate measurement.

Fig. 4 represents typical histograms of the rupture forces obtained for the streptavidin–maleimide in (a) a pH 7.4 phosphate buffer solution at the loading rate of 1115 pN s^{-1}, (b) a pH 7 sodium nitrate solution at the loading rates of 1447 pN s^{-1} and (c) a pH 10 carbonate buffer solution at the loading rates of 1382 pN s^{-1}, and for the avidin–maleimide in (d) a pH 7.4 phosphate buffer solution at the loading rate of 558 pN s^{-1}, (e) a pH 7 sodium nitrate solution at the loading rates of 678 pN s^{-1} and (f) a pH 10 carbonate buffer solution at the loading rates of 680 pN s^{-1}. The modal rupture forces were obtained by fitting using eqn (1) based on the DFS method.

Fig. 5 shows the relationships between the modal rupture force and the logarithm of the loading rate obtained in 0.01 M phosphate buffer solution (pH 7.4), 0.05 M sodium nitrate solution (pH 7) and 0.05 M carbonate buffer solution (pH 10).

For streptavidin (Fig. 5(a)), formations of a large potential barrier position (0.68 ± 0.01 nm) in the phosphate buffer solution and a short (0.26 ± 0.01 nm) potential position in the sodium nitrate solution, which were observed in the previous study,[23–25]
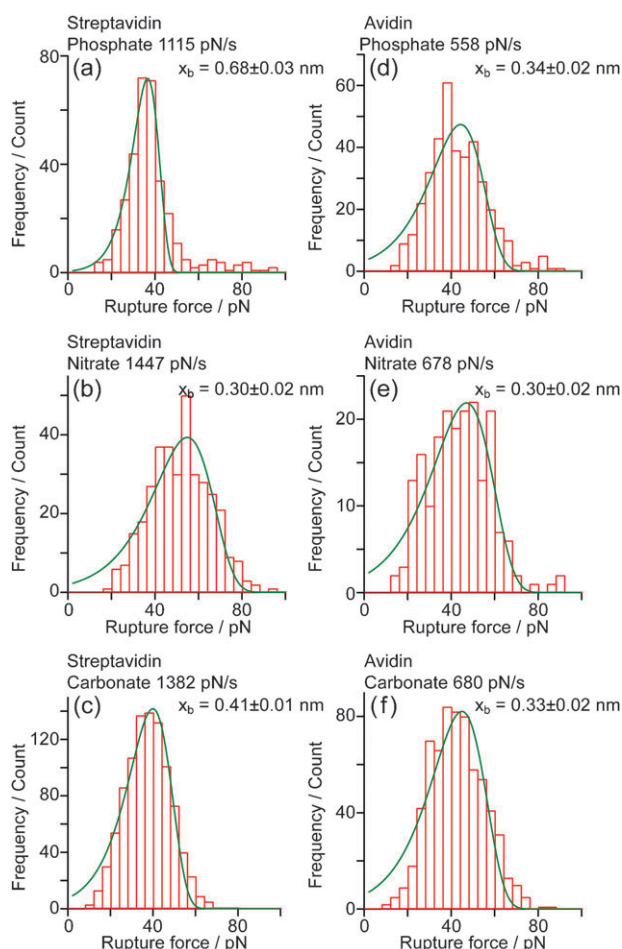
Fig. 4 Typical histograms of the rupture forces obtained for the streptavidin–maleimide and avidin–maleimide structures in phosphate, sodium nitrate and carbonate buffer solutions at certain loading rates. The solid green lines show the theoretical fitting curves obtained using eqn (1), from which the modal rupture forces are obtained. In addition to the analysis of the slope of Fig. 5, potential barrier positions x_b can be estimated by analyzing the shape of the rupture force distribution.[21–25] The potential barrier positions x_b obtained from each distribution in Fig. 4, using the method discussed in ref. 23–25, are shown in the figures.
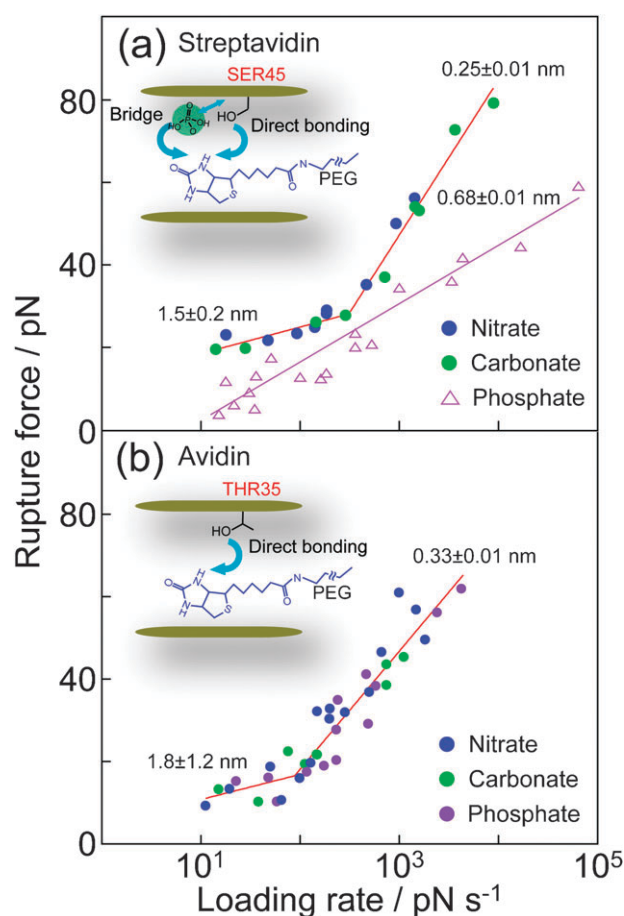

Fig. 5 Relationship between the modal rupture force and the logarithm of the loading rate obtained for (a) streptavidin–biotin and (b) avidin–biotin complexes. Colored lines are slopes for indication, and the potential positions shown together are those obtained from the slopes. The lines with two components in (a) and (b) represent the results of fitting all the data including those obtained in nitrate and carbonate buffer solutions, respectively. The potential barrier positions at middle reaction sites obtained from the data for each solution are summarized in Table 1.

have been confirmed again. In addition, a similar short potential barrier position (0.24 ± 0.01 nm) was observed also in the carbonate buffer solution.

Here, since the distance between the inner and outer sites is about 1 nm, the bonds with a potential barrier position larger than 1 nm (indicated by the slopes of 1.5 ± 0.2 nm and 1.8 ± 1.2 nm in Fig. 5(a) and (b), respectively) are not clear. In the pioneering work by Merkel et al.[7] using phosphate buffer solution, they observed a potential barrier longer than 1 nm (~3 nm) only for avidin.[7] In our experiment, we also observed this long potential barrier position only for avidin for phosphate buffer solution, which is in good agreement with Merkel et al.'s results.[7]

On the other hand, the long potential barrier positions were commonly observed for streptavidin and avidin in nitrate and carbonate buffer solutions. However, since the distance between the inner and outer reaction sites is about 1 nm,

further study is needed to clarify the mechanism of the interactions to provide the large potential barrier positions. We leave this issue for future study.

The potential barrier position of 0.68 ± 0.01 nm formed in the phosphate solution is close to the value obtained in 0.05 M ammonium sulfate solution for streptavidin (Fig. 6). Similar to the results obtained in a phosphate solution, only one potential barrier position, estimated at 0.66 ± 0.03 nm, was observed, which was confirmed by X-ray diffraction method to be a bridged bond formed by SO_4^{2-} between biotin and amino acid residues SER45 and SER27 of the streptavidin molecule.[2]

These results support the fact that the streptavidin–biotin bond made in a phosphate buffer solution is a bridge bond formed by phosphate buffer molecules.

On the other hand, the barrier positions observed in the sodium nitrate and carbonate buffer solutions (see Table 1) are consistent with that obtained by MD calculation for the direct bond between SER45 and the ureido oxygen of biotin (0.26 nm).[28] In general, a protein causes denaturation through
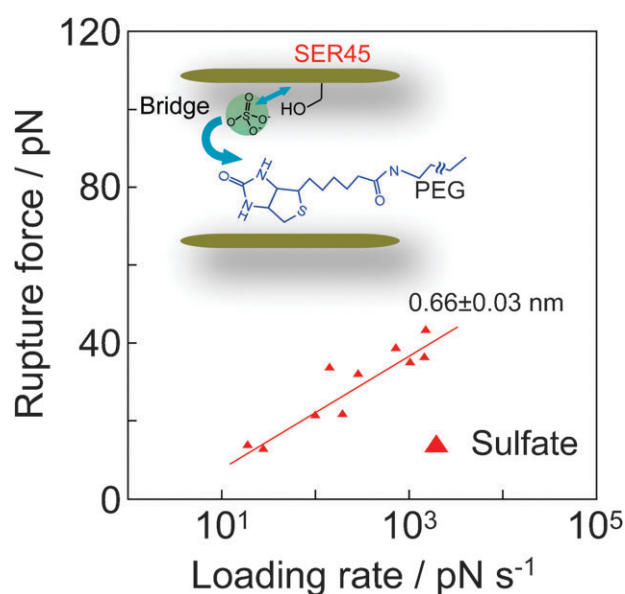
Fig. 6 Relationship between the modal rupture force and the logarithm of the loading rate obtained for streptavidin–biotin in a 0.05 M ammonium sulfate solution (pH 5).

the change in pH and ionic strength. Therefore, it may be considered that the binding potential is changed by denaturation. However, as the protonation due to the change in pH was observed at TYR43[2] in a previous study, the reaction sites that may change the potential barrier are the inner binding sites of the amino acid residues such as TYR43, ASN23, ASP128 and SER27, which are not probed here because of the fixed condition of the streptavidin and avidin molecules prepared with maleimide molecules used in this experiment.[13] In fact, the observed values of the potential positions were independent of pH, supporting the results obtained in this study.

These results indicate that, for streptavidin, both bridged and direct hydrogen bonds can be formed at the middle binding sites depending on the buffer solution, *i.e.*, bridged bonds (via phosphate molecules) in a phosphate solution and direct hydrogen bonds in other (nitrate or carbonate) solutions, respectively.

For avidin, in contrast to the reaction processes observed for streptavidin, completely different results were obtained, that is, although the direct hydrogen bond of 0.12 nm,[7–9]

Table 1 Potential barrier positions in potential landscapes for the formation of the bonds of a biotin molecule with the middle bonding sites of streptavidin and avidin in various buffer solutions

	pH	Fix type	Buffer molecule	Potential barrier position/nm
Streptavidin	7	Maleimide	Nitrate	0.26 ± 0.01
	10		Carbonate	0.24 ± 0.01
	5		Sulfate	0.66 ± 0.03
	7.4		Phosphate	0.68 ± 0.01
	7.4	PEG[23,24]	Phosphate	0.63 ± 0.03
	6.8	PEG[7]	Phosphate	0.5
Avidin	7	Maleimide	Nitrate	0.32 ± 0.01
	10		Carbonate	0.35 ± 0.03
	7.4		Phosphate	0.33 ± 0.01
	6.8	PEG[7]	Phosphate	0.3

which is formed at the inner sites and should not be probed in the experimental condition here, disappeared as expected, the barrier position showed no marked change in any of the three solutions. The potential barriers at 0.32 ± 0.01 nm in a sodium nitrate solution, 0.35 ± 0.03 nm in a carbonate solution and 0.33 ± 0.01 nm in a phosphate solution (see Table 1) are close to each other, the values of which are close to the result obtained in a previous study, 0.3 nm in a phosphate solution.[7,8]

The potential barrier position x_b can also be estimated by analyzing the shape of rupture force distribution.[21–25] The solid green lines in Fig. 4 show theoretical fitting curves obtained using eqn (1), and the potential barrier positions x_b obtained from each distribution in Fig. 4 are (a) 0.68 ± 0.03 nm, (b) 0.30 ± 0.02 nm, (c) 0.41 ± 0.01 nm, (d) 0.34 ± 0.02 nm, (e) 0.30 ± 0.02 nm and (f) 0.33 ± 0.02 nm. These results are consistent with the barrier positions obtained from the slope of Fig. 5; the values are close to 0.7 nm for streptavidin in phosphate buffer solution and to 0.3 nm in other cases.

The results obtained for the bonding at the middle sites are summarized in Table 1, where the data for each solution in Fig. 5 were analyzed separately. For comparison, the results reported in ref. 7, 23 and 24 are also shown.

What causes the observed variation in the bonding processes? First, the origin of the variation between molecular bridging and direct hydrogen bonding observed for streptavidin is considered to be the structure of the ion species in the solutions. Since phosphate and sulfate have a tetrahedral structure, the mechanism may be related to the structure of the buffer molecules, *i.e.*, when buffer molecules have a tetrahedral structure consisting of four oxygen atoms, a molecular bridging is induced between SER45 and the biotin molecule,[2] and a direct hydrogen bonding is induced between SER45 and the biotin molecule for a buffer molecule with a trigonal structure. Further experiment is in progress.

On the other hand, the difference in the type of amino acid residues in the middle sites of the two molecules, namely, SER45 and THR35 (Fig. 1), produces the difference observed for streptavidin and avidin. Since the values observed for avidin are similar and independent of the type of buffer solution used, these values are attributed to those of the potential barriers formed by direct hydrogen bond between the biotin molecule and the middle reaction sites of avidin, such as THR35. Note that the barrier positions of the direct hydrogen bonds observed for streptavidin are shorter than those for avidin, which probably originates from the difference in the type of amino acid residues. A theoretical analysis including finer structures of amino residues and buffer molecules is necessary.

4. Conclusions

By site-selective DFS analysis,[23–25] effects of the local variation in the type of amino acid residues in streptavidin and avidin molecules on their reaction dynamics with a biotin molecule were studied at the single molecule level, and critical effects, which had been hidden behind the averaged function, have been revealed, for the first time. The slight difference between the local structures of amino acid residues at the

12582 | *Phys. Chem. Chem. Phys.,* 2010, **12**, 12578–12583

This journal is © the Owner Societies 2010

middle sites, SER45 and THR35 for streptavidin and avidin, respectively, strongly affects the microscopic reaction processes, *i.e.*, the variation governs the type of bond as well as the fine structure of the potential landscape. For streptavidin, a bridged or direct hydrogen bond is induced depending on the molecular structure in the buffer solution. For avidin, in contrast, only a direct hydrogen bond is observed for all the buffer solutions used in the experiment. Since final functions in a system are realized through the assembly of local effects, the obtained results indicate the importance of analyzing the reaction processes with respect to the local structures of molecules, for further development of nanoscale functional devices.

Acknowledgements

References

1 P. C. Weber, D. H. Ohlendorf, J. J. Wendoloski and F. R. Salemme, *Science*, 1989, **243**, 85.
2 B. A. Katz, *J. Mol. Biol.*, 1997, **274**, 776.
3 T. Huberman, Y. Eisenberg-Domovich, G. Gitlin, T. Kulik, E. A. Bayer, M. Wilchek and O. Livnah, *J. Biol. Chem.*, 2001, **276**, 32031.
4 S. Yasuda, I. Suzuki, K. Shinohara and H. Shigekawa, *Phys. Rev. Lett.*, 2006, **96**, 228303.
5 T. A. Sulchek, R. W. Friddle, K. Langry, E. Y. Lau, H. Albrecht, T. V. Ratto, S. J. DeNardo, M. E. Colvin and A. Noy, *Proc. Natl. Acad. Sci. U. S. A.*, 2005, **102**, 16638.
6 G. Neuert, C. Albrecht, E. Pamir and H. E. Gaub, *FEBS Lett.*, 2006, **580**, 505.
7 R. Merkel, P. Nassoy, A. Leung, K. Ritchie and E. Evans, *Nature*, 1999, **397**, 50.
8 E. Evans, *Faraday Discuss.*, 1998, **111**, 1.
9 C. Yuan, A. Chen, R. Kolb and V. T. Moy, *Biochemistry*, 2000, **39**, 10219.
10 A. B. Patel, S. Allen, M. C. Davies, C. J. Roberts, S. J. B. Tendler and P. M. Williams, *J. Am. Chem. Soc.*, 2004, **126**, 1318.
11 M. O. Piramowicz, P. Czuba, M. Targosz, K. Burda and M. Szymoński, *Acta Biochim. Pol.*, 2006, **53**, 93.
12 J. Wong, A. Chilkoti and V. T. Moy, *Biomol. Eng.*, 1999, **16**, 45.
13 E. Evans and K. Ritchie, *Biophys. J.*, 1999, **72**, 1541.
14 E. Evans and K. Ritchie, *Biophys. J.*, 1999, **76**, 2439.
15 F. Pincet and J. Husson, *Biophys. J.*, 2005, **89**, 4374.
16 J. Husson and F. Pincet, *Phys. Rev. E*, 2008, **77**, 026108.
17 T. Strunz, K. Oroszlan, I. Schumakovitch, H.-J. Güntherodt and M. Hegner, *Biophys. J.*, 2000, **79**, 1206.
18 O. K. Dudko, G. Hummer and A. Szabo, *Proc. Natl. Acad. Sci. U. S. A.*, 2008, **105**, 15755.
19 O. K. Dudko, J. Mathé, A. Szabo, A. Meller and G. Hummer, *Biophys. J.*, 2007, **92**, 4188.
20 F. Rico and V. T. Moy, *J. Mol. Recognit.*, 2007, **20**, 495.
21 C. Ray, J. R. Brown and B. B. Akhremitchev, *Langmuir*, 2007, **23**, 6076.
22 O. Björnham and S. Schedin, *Eur. Biophys. J.*, 2009, **38**, 911.
23 A. Taninaka, O. Takeuchi and H. Shigekawa, *Appl. Phys. Express*, 2009, **2**, 085002.
24 A. Taninaka, O. Takeuchi and H. Shigekawa, *Int. J. Mol. Sci.*, 2010, **11**, 2134.
25 O. Takeuchi, T. Miyakoshi, A. Taninaka, K. Tanaka, D. Cho, M. Fujita, S. Yasuda, S. P. Jarvis and H. Shigekawa, *J. Appl. Phys.*, 2006, **100**, 074315.
26 A. F. Oberhauser, P. K. Hansma, M. C. Vazquez and J. M. Fernandez, *Proc. Natl. Acad. Sci. U. S. A.*, 2001, **98**, 468.
27 P. E. Marszalek, H. Li, A. F. Oberhauser and J. M. Fernandez, *Proc. Natl. Acad. Sci. U. S. A.*, 2002, **99**, 4278.
28 J. Zhou, L. Zhang, Y. Leng, H.-K. Tsao, Y.-J. Sheng and S. Jiang, *J. Chem. Phys.*, 2006, **125**, 104905.